Applied Clay Science 99 (2014) 254–260

Contents lists available at ScienceDirect

Applied Clay Science

journal homepage: www.elsevier.com/locate/clay

Research paper

Modification of bentonite by combination of reactions of acid-activation, silylation and ionic exchange

David A. D'Amico [1], Romina P. Ollier [1], Vera A. Alvarez [1], Walter F. Schroeder *, Viviana P. Cyras *

Institute of Materials Science and Technology (INTEMA), University of Mar del Plata, Av. Juan B. Justo 4302, 7600 Mar del Plata, Argentina

ARTICLE INFO

Article history:
Received 7 March 2014
Received in revised form 26 June 2014
Accepted 2 July 2014
Available online 30 July 2014

Keywords:
Bentonite
Acid-activation
Cationic exchange
Grafting

ABSTRACT

Objective: The aim of this study is to analyze different strategies of modification of bentonite (Bent) combining reactions of cationic exchange, silylation and acid activation.
Methods: Six samples of modified bentonite were prepared: silylated bentonite (S-Bent), acid-activated bentonite (A-Bent), exchanged clay (E-Bent), silylated and acid-activated clay (S–A-Bent), exchanged and acid-activated clay (E–A-Bent), and exchanged, silylated and acid-activated bentonite (E–S–A-Bent). To study the effectiveness of the different treatments, X-ray diffraction analysis, thermogravimetric analysis, Fourier transform infrared spectroscopy and water absorption tests were performed.
Results: The silylated bentonite presented a significant reduction in the equilibrium water uptake percentage with respect to the unmodified clay, even when small amounts of silane were incorporated to the clay. On the other hand, no significant changes in the organic content were obtained when the silylation reaction was performed on previously acid-activated bentonite. When a sample of silylated and activated bentonite was further modified by cationic exchange reaction, it was found that the previous treatments allowed increasing the uptaken amount of surfactant cations during the exchange reaction. In fact, the combination of the three treatments (acid-activation, silylation and cationic exchange) gave place to the modified bentonite with the biggest basal spacing and the lower equilibrium water uptake percentage.
Significance: The results obtained in the present study reveal the potential usefulness of the E–S–A-Bent sample as promising filler for the formulation of clay polymer nanocomposites. Work is in progress in this direction.

1. Introduction

Polymeric materials have been reinforced with different fillers (Bergaya et al., 2011a, 2013; Limpanart et al., 2005; Roelofs and Berben, 2006; Xie et al., 2002) with the aim of improving specific properties, mainly thermal, barrier, impact and mechanical, for an important number of applications (Lambert and Bergaya, 2013). There are several factors that determine the final performance of a nanocomposite material, such as the properties of each component, volume fraction, aspect ratio, orientation of the filler and the filler/matrix interface, which is mainly determined by the chemical compatibility between both components and the processing method used to obtain the nanocomposite. In a great number of cases, the interaction between both components is not strong enough to reach the desired properties.

It is known that macro and micro-sized fillers generally present structural defects, and that the amount of defects markedly decreases when the dimensions of the filler are reduced to molecular (nano) size. Nevertheless, as the size of the filler turns into smaller, the tendency to agglomerate inside the matrix increases (Drown et al., 2007). Among the nano-sized fillers, clays are one of the most used for making polymer based nanocomposite materials (Bergaya et al., 2013; Drown et al., 2007; Fornes et al., 2001; Hedley et al., 2007; Mandalia and Bergaya, 2006). The clays are layered inorganic phyllosilicates where the layers of about 1 nm in thickness are held apart mainly by electrostatic forces (Bergaya et al., 2011a; Mandalia and Bergaya, 2006). The crystalline structure of clays is formed by bi-dimensional layers where a central octahedral layer of either, alumina or magnesia, is attached to two external tetrahedrons of silica in such a way that the oxygen ions of the octahedral layer also belong to the tetrahedral layers (Alexandre and Dubois, 2000; Bergaya et al., 2011a; Picard et al., 2007). Two important clays, due to environmental and economic relevance and mechanical and chemical resistance, are bentonite and montmorillonite (Bergaya et al., 2012; He et al., 2006; Mandalia and Bergaya, 2006; Zampori et al., 2008). Bentonites are important due to their chemical and physical properties, characterized for a moderate negative charge.

The possibility of producing a clay polymer nanocomposite (CPN) with really improved properties is restricted by the morphology of the

* Corresponding authors. Tel.: +54 223 481 66 00; fax: +54 223 481 00 46.
E-mail addresses: wschroeder@fi.mdp.edu.ar (W.F. Schroeder), vpcyras@fi.mdp.edu.ar (V.P. Cyras).
[1] Tel.: +54 223 481 66 00; fax: +54 223 481 00 46.

http://dx.doi.org/10.1016/j.clay.2014.07.002
0169-1317/

produced material. For that purpose, an exfoliated structure, in which the silicate layers are completely and uniformly dispersed in a continuous polymeric matrix (Bergaya et al., 2013; Roelofs and Berben, 2006), should be obtained. However the particles tend to agglomerate making difficult to obtain such a kind of nanostructure. The different polar character of clays (mostly hydrophilic) and polymeric matrices (mainly hydrophobic) make necessary modification in one of them in order to increase the chemical compatibility between both components, so as to improve the dispersion of the clay, and consequently the final properties (Bergaya et al., 2012; Čapková et al., 2006).

The first step in obtaining clay-based products with homogeneous structure is the preparation of stable suspensions. In addition, the compatibility of clay with matrix is very important (Tunç et al., 2012). There are different methods of increasing the clay matrix compatibility. The most popular one is based on the conversion of these hydrophilic silicates in organophilic ones, via an ionic exchange reaction (Bergaya et al., 2011b, 2012; Picard et al., 2007; Xi et al., 2007; Xie et al., 2002). In these kinds of reactions, the hydrated sodium cations, which are placed in the interlayer space, are replaced by other positively charged surfactants such as alkyl ammonium or phosphonium cations with long alkyl chains (Picard et al., 2007; Xi et al., 2007; Xie et al., 2002). After this treatment, the basal spacing of the layers increases (Xi et al., 2004) and the modified clay has less surface energy and is more compatible with hydrophobic polymers (Drown et al., 2007; Picard et al., 2007).

The activation of clay includes a wide range of chemical treatments. During acid activation, the edges of the crystals are opened and the Al^{3+} and Mg^{2+} cations of the octahedral sheet become soluble. The treatment with mineral acid is also known to impart surface acidity of the clay, which improves its catalytic properties (Bergaya et al., 2011b; Breen et al., 1995; Frost et al., 2001; Komadel and Madejová, 2006; Kristof et al., 2002; Mortland et al., 1986; Pinnavaia, 1983). Also, the acid activation of smectites or bentonites is used before cation exchange reactions.

More recently, the possibility of grafting silane molecules on the surface of the clay layers has been studied (Bergaya et al., 2011b; He et al., 2013; Herrera et al., 2004; M. Park et al., 2004). The reactive –OH groups are present in two main places: at the edges and at the structural defects (Di Gianni et al., 2008; He et al., 2005a; Van Olphen, 1977), so that, the functionalization can take place at three possible sites: at the interlayer space, at the external surface (Herrera et al., 2004) and at the edges (Bergaya et al., 2011b; M. Park et al., 2004). The reaction of silylation at the interlayer and at the edges –OH groups can increase the interlayer space of clays (Isoda et al., 2000; K.-W. Park et al., 2004). It is also possible to produce the silylation reaction on clays modified by ion exchange (Chen and Yoon, 2005a, 2005b, 2005c).

Several previous studies have described the effects of different modification methods of clays with the aim of increasing the clay matrix compatibility. Less attention has been paid to explore how one modification method affects the further modification by other methods (Fernández et al., 2013). In fact, as far as the authors are aware, there is no previous study in the vast literature of clay modification analyzing the effect of different previous treatments, such as silylation and/or acid activation, on the cationic exchange reaction employing alkyl phosphonium salts; which, as it is known, present higher thermal stability than the traditional quaternary ammonium cations (Bergaya et al., 2011b; Xie et al., 2002). In the present study, several strategies of modification of Bent combining reactions of cation exchange, silylation and acid activation are analyzed. The effectiveness of each strategy is discussed to the light of the characterization results by X-ray diffraction analysis, thermogravimetric analysis, Fourier transform infrared spectroscopy and water absorption tests.

2. Experimental

2.1. Materials

The clay employed in this work was a bentonite supplied by Minarmco S.A. (Neuquén, Argentina). The cation exchange capacity (CEC) of bentonite was found to be 0.939 meq/g as measured by the methylene blue method. The dimethyloctadecylchlorosilane (DMOCS) and tributylhexadecylphosphonium bromide (TBHP) organic modifiers as well as pyridine (anhydrous, 99.8%) were purchased from Aldrich and used as received. Other solvents were purified by conventional drying and distillation procedures.

2.2. Silylation reaction

A 350 mL volume of anhydrous n-butanol was introduced in a 500 mL two-neck round bottom flask. 1.5 g of Bent (previously dried in an oven at 110 °C overnight) was then added to the solvent together with an excess of DMOCS (5 g). The mixture was heated at 100 °C and kept under gentle stirring. After 15 min, 3.5 mL of pyridine was added to the mixture and it was refluxed for 24 h. The product was collected by filtration, and then washed three times with n-butanol and once with ethanol. Finally, the product was dispersed in 20 mL of ethanol and dried in an oven at 80 °C for 24 h.

2.3. Acid activation

A 5 g portion of Bent was dispersed in 200 mL of water. Then 10 mL of 98% (w/w) H_2SO_4 was added and the mixture was stirred at room temperature for 6 h. An acid/clay (w/w) ratio of 3.6 was calculated using the dry mass of clay and 98% H_2SO_4. The dispersion was then centrifuged in order to separate the acid-activated clay. Once separated, the clay was washed with aliquots of 30 mL of distilled water and centrifuged at 10,500 rpm for 10 min. This procedure was repeated several times until reaching a pH value equal to 6. Finally, the wet acid-activated Bent was frozen for 24 h and then lyophilized at 100 mTorr and −50 °C for 72 h using a VirTis 2KBTES-55 freeze dryer.

2.4. Ion exchange

A 2.5 g sample of clay was dispersed in 100 mL of distilled water and 1.1 g of tributylhexadecylphosphonium bromide (TBHP) was added. The dispersion was kept under stirring at the temperature of 70 °C for 4 h. The clay was then filtered and washed several times with distilled water until no more trace of TBHP was found by FTIR analysis of the filtrate. Finally, the exchanged clay was dispersed in ethanol and dried in an oven at 80 °C for 24 h.

2.5. Characterization

X-ray diffraction (XRD) analysis was performed on the clay powders using an X-Pert pro diffractometer, operating at 40 kV and 40 mA, with CuKα radiation (λ = 1.54 Å), at a scanning speed of 1.5°/min. The basal spacing distances (d_{001}) were calculated from the 2θ values using the Bragg equation. The diffractogram of the raw Bent was analyzed using the X'Pert HighScore 2.2d software.

Elemental analysis was performed by X-ray Fluorescence (XRF) spectroscopy using a PANalytical MiniPal 2, with Cr Kα radiation (λ = 0.2291 nm), 20 kV and 5 μA, in helium flow. Light elements (below Na in periodic table) could not be detected.

Thermogravimetric analysis (TGA) was carried out with a Shimadzu thermal analyzer at a heating rate of 10 °C/min from room temperature to 700 °C in nitrogen flow. The specimen mass was in the range of 7–15 mg.

Fourier transform infrared (FTIR) spectra were acquired with a Nicolet 6700 Thermo Scientific instrument, over the range of 400–4000 cm^{-1} from 32 co-added scans at 4 cm^{-1} resolution.

Water absorption tests were carried out at 90% RH (relative humidity). To control the humidity level during testing, the clay samples were enclosed in a small chamber containing an aqueous solution of glycerine (34 w/w%) which fixes the relative humidity (RH) within 90 ± 1% (Greenspan, 1977). Before tests, all the samples were dried under vacuum until constant mass. Samples were weighted at prefixed times and the water absorption at each time was calculated as:

$$M_t(\%) = \frac{M_t - M_0}{M_0} \cdot 100 \quad (1)$$

where M_t is the mass of the sample at a time t and M_0 is the initial mass of the sample (dried).

3. Results and discussion

The raw Bent used in this study consisted predominantly of montmorillonite as evidenced by X-ray diffraction (XRD) analysis (see Supplementary material). It contained quartz and feldspar as major impurities, as well as traces of gypsum and sepiolite. The basal spacing of the raw Bent was 1.3 nm, and its cation exchange capacity (CEC) was found to be 0.939 meq/g.

3.1. Silylation of bentonite (S-Bent)

The hydroxyl groups present on the surface of the clay layers act as active sites which can be used to functionalize the clay platelet surface. The grafting of silane molecules on the surface of the clay layers has been reported in the literature concerning the functionalization of silica particles and their compatibilization with organic matrices (Di Gianni et al., 2008; He et al., 2005a, 2013; Herrera et al., 2004; M. Park et al., 2004; Van Olphen, 1977). In the present study, dimethyloctadecylchlorosilane (DMOCS) is used for this purpose so that, while the chlorosilane group can react with the active sites on the clay surface, the alkyl chain can take part in the compatibility of the clay with the polymeric matrix.

When a monochlorosilane is used for silylation, the reaction between chloro and surface hydroxyl groups is very sluggish as a consequence of the steric hindrance of the bulky methyl groups of the chlorosilane. This reaction can be promoted by using a base like triethylamine, butylamine, or pyridine as a catalyst (Tripp and Hair, 1993). The base reacts with the chlorosilane to form a penta-coordinated silicon intermediate. The Si – Cl bond is lengthened in the intermediate, which then reacts with the surface hydroxyl groups to form Si – O – Si covalent bonds. A second mechanism has also been proposed for the nucleophile-catalyzed silylation reaction (Tripp and Hair, 1993). The base attaches directly to the silanols on the surface of the clay layers increasing in this way the nucleophilic character of the Si – O group, which then attacks the Si atom of the silane molecules forming Si – O – Si bonds. In the present work, pyridine has been used as a nucleophilic catalyst to promote the condensation reaction between the silane and the surface hydroxyl groups.

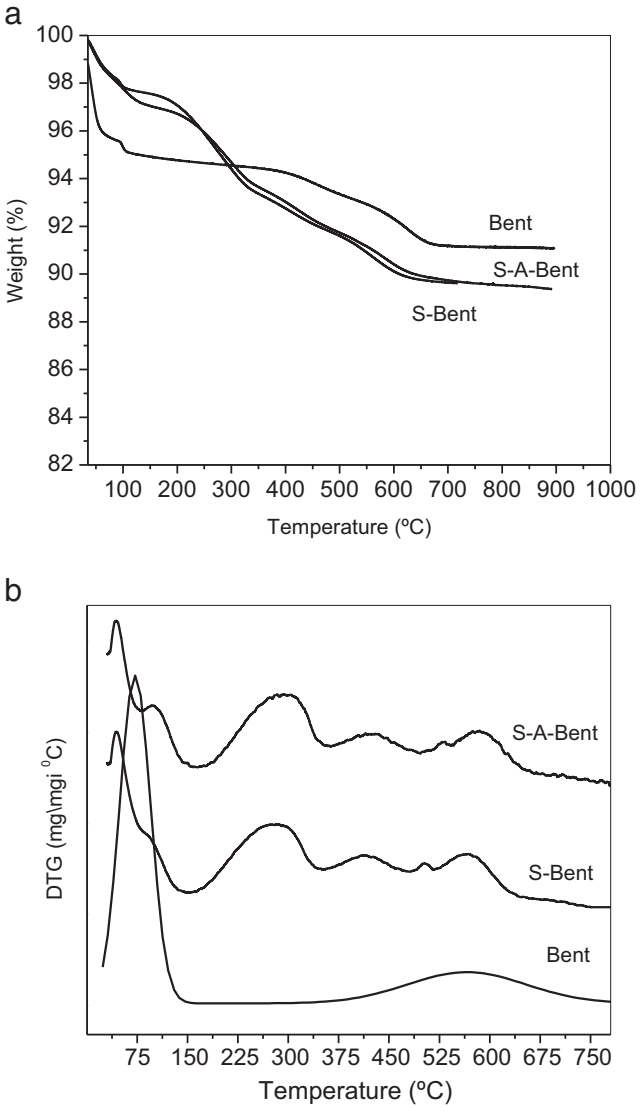

Fig. 2. a. TGA curves of Bent, S-Bent and S–A-Bent. b. DTG curves of Bent, S-Bent and S–A-Bent.

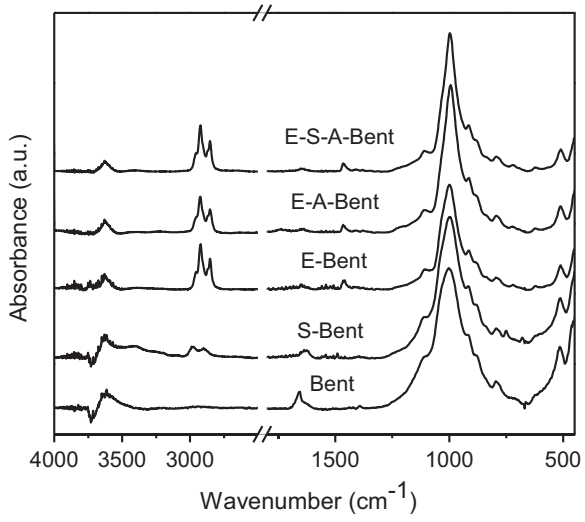

Fig. 1. FTIR spectra of Bent and modified bentonites.

The comparison between the FTIR spectrum of the pure Bent and the spectrum of the Bent after the silylation reaction with DMOCS (S-Bent) is shown in Fig. 1. The appearance of absorption bands at 2987 and 2900 cm^{-1} assigned to antisymmetric ($\nu_{as}(CH_2)$) and symmetric ($\nu_s(CH_2)$) stretching vibrations of the methylene groups introduced by the DMOCS indicates the existence of silane in the S-Bent.

Thermogravimetric analysis (TGA) was performed on these materials to obtain information on their degradation and evaluate the amount of silane incorporated by the silylation reaction. The TGA curves for Bent and S-Bent are shown in Fig. 2a, whereas the corresponding first derivatives (DTG) are shown in Fig. 2b. The DTG curve of Bent

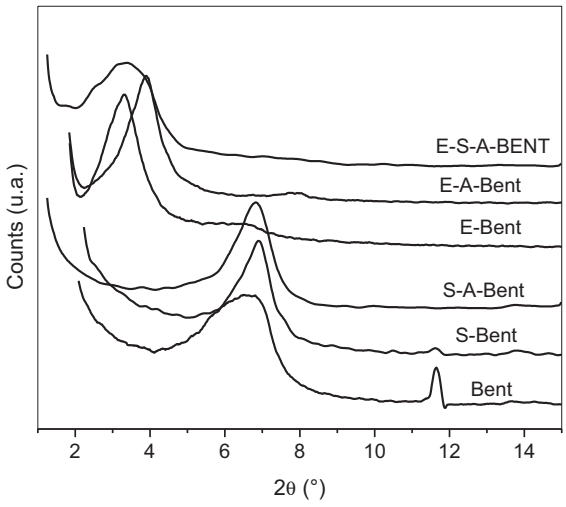

Fig. 3. X-ray diffraction patterns of Bent and modified bentonites.

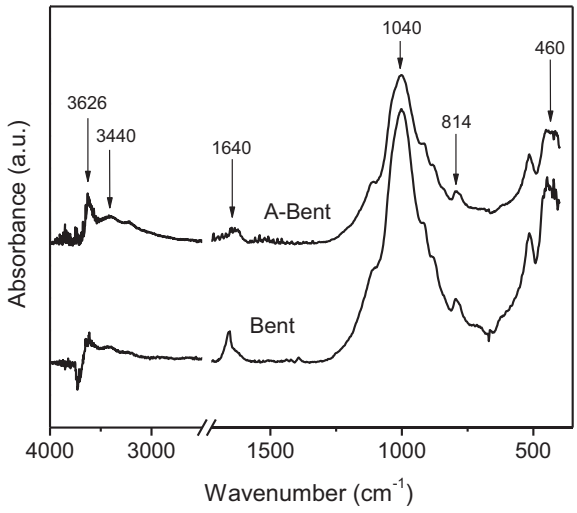

Fig. 4. FTIR spectra of Bent and A-Bent.

displays two peaks at 70 and 570 °C corresponding to loss of the physically adsorbed water and dehydroxylation of clay, respectively (Di Gianni et al., 2008; Zhang et al., 2006). The DTG curve of S-Bent displays peaks at 60, 280, 390, 500 and 565 °C. As the Bent sample is thermally stable in the temperature range of 150–500 °C, the mass loss in this region should be attributed to loss of the silane. It has been reported in the literature that the organosilyl groups grafted to the silicates present high thermal stability and start to decompose only at 400 °C (Zhang et al., 2006). Hence, the peaks at 280 and 390 °C are attributed to the decomposition of the intercalated silane within the interlayer spaces of bentonite, while the peak at 500 °C is assigned to the decomposition of the grafted silane. To test this assignation, we prepared a Bent sample treated with DMOCS in the same conditions, but without the addition of pyridine. The DTGA spectrum of this sample presents peaks between 180 and 390 °C due to the presence of intercalated silane, but it does not present peak at 500 °C since the silane has not been grafted (see Supplementary material). This result reveals that the silylation reaction took place in the S-Bent sample. The comparison of the TGA curves corresponding to the Bent and S-Bent samples (Fig. 2a) reveals that there is 4.3 w/w% of organic content in the S-Bent, as listed in Table 2.

The X-ray diffraction patterns for Bent and its silylated derivative (S-Bent) are shown in Fig. 3. Bent exhibits a strong reflection at $2\theta = 6.8°$ corresponding to a basal spacing of 1.31 nm (see Table 2). There is almost no change in the position of the 001 reflection (basal reflection) for S-Bent ($2\theta = 6.9°$), as seen in Fig. 3. This result indicates that the silylation reaction has had a negligible effect on the basal spacing of the Bent. In the literature, both experimental studies and molecular modeling displayed the basal spacing at 1.3–1.5 nm when the arrangement of the intercalated organic molecules was a lateral-monolayer (Bergaya et al., 2011b; He et al., 2005b). On the basis of this argument, it is proposed that the monolayer arrangement model is adopted for DMOCS within the bentonite interlayer space.

A remarkable feature of the silylated derivative is that it presents a significant reduction in the equilibrium water uptake percentage with respect to the unmodified clay (Table 2). In fact, the Bent sample after several days in a 90% relative humidity environment absorbs 17.4 w/w% of water, while this value is reduced to 5.2 w/w% for the S-Bent. This result is an indication that the S-Bent is much less hydrophilic than those of neat Bent. A reduction in the hydrophilicity of the clay normally results in higher clay polymer compatibility, which is one of the key factors to obtain CPN with desired properties.

3.2. Silylation of acid-activated bentonite (S–A-Bent)

In this section, a different modification strategy is reported. The bentonite was first activated (A-Bent) by treatment with mineral acid, and then silylated (S–A-Bent). The treatment of the clay with mineral acid (e.g. acid activation) dissolves impurities such as calcite, opens the edges of the platelets and consequently increases the surface area and the pore diameters (Kooli, 2008). In addition, exchangeable cations are replaced by protons increasing in this way the amount of –OH groups available for further functionalization.

FTIR spectra of the natural and acid-activated bentonite are shown in Fig. 4, where changes in the characteristic signals of hydroxyl groups and the silicate anions can be observed. The Bent and A-Bent exhibit bands at 3440 and 1640 cm^{-1} assigned to the stretching and bending vibrations for the hydroxyl groups of water molecules present in the clay samples. It can be seen a diminution in the intensity of the bands at 1040 cm^{-1} (Si–O stretching), 814 cm^{-1} (O–Si–O asymmetric stretching) and 460 cm^{-1} (Si–O–Si bending) due to changes in the Si environment produced by acid attack, indicating textural changes in the A-Bent. The increase in intensity of the peak at 3626 cm^{-1} due to O–H stretching vibrations suggests that exchangeable cations have been replaced by protons during acid treatment increasing in this way the amount of available –OH groups. These results are in accord with the XRF data, which revealed a significant reduction in the amount of CaO in the A-Bent regarding to the raw Bent, as a result of partial dissolving of calcium ions during the acid activation treatment (see Table 1). It is worth mentioning that sodium and other light elements cannot be detected by the XRF equipment.

The acid-activated bentonite was then silylated with dimethyloctadecylchlorosilane (DMOCS) using pyridine as a catalyst.

Table 1
Chemical composition of raw and treated bentonites.

Sample	Composition (wt.%)								
	SiO_2	Al_2O_3	Fe_2O_3	MgO	CaO	K_2O	TiO_2	P	Others[a]
Raw Bent	52.3	13.1	22.1	1.9	4.7	1.3	2.0	0	2.4
A-Bent	55.2	14.7	22.5	2.0	1.8	1.3	2.1	0	0.5
S–A-Bent	55.2	14.7	22.5	2.0	1.8	1.3	2.1	0	0.5
E–A-Bent	57.2	15.1	19.2	2.0	1.5	1.0	2.2	1.9	0
S-Bent	53.8	14.0	21.8	1.2	3.3	1.4	2.2	0	1.4
E-Bent	52.0	15.3	22.4	1.8	3.1	1.3	2.0	2	0
E–S–A-Bent	53.8	15.1	23.2	1.7	1.4	1.1	2.1	1.7	0

[a] Others = % SO_3 + % Cl.

Table 2
Effect of several treatments on the relevant characteristics of bentonite (Bent).

Bent		Property	
Treatment	d_{001} (nm)	Organic content (%)	M_{final} (%)
None	1.3	0.0	17.4
S	1.3	4.3	5.2
S–A	1.3	4.3	5.6
E	2.7	18.8	2.8
E–A	2.3	18.4	3.4
E–S–A	2.6	26.7	2.6

S: silylation with excess of DMCOS.
A: activation.
E: cation exchanged.
d_{001}: interlaminar spacing from XRD.
Organic content (%): weight change percentage calculated from TGA curves.
M_{final}: equilibrium water uptake percentage measured in a 90% RH environment.

With the goal of evaluating the effect of the activation treatment on the posterior silylation process, the amount of intercalated and grafted silane was assessed by performing thermogravimetric analysis. The TGA curve for the silylated activated bentonite (S–A-Bent), in comparison with Bent and S-Bent, is shown in Fig. 2a. There is a clear similarity between the thermogravimetric profiles of S-Bent and S–A-Bent. Comparing the first derivatives of the TGA curves for these samples (Fig. 2b), both present two peaks at 280 and 390 °C attributed to the decomposition of the intercalated silane, and a weaker peak at about 500 °C ascribed to the decomposition of grafted silane. Moreover, the total organic content within the interlayer spaces of S–A-Bent (4.3 w/w%) was almost the same than for S-Bent, as seen in Table 2.

Complementary information obtained from XRD analysis is in agreement with the previous results. The X-ray diffraction pattern for S–A-Bent in comparison with those of S-Bent and Bent is shown in Fig. 3, and the calculated value for the basal spacing is listed in Table 2. No significant changes were observed in the position of the 001 reflection for the S–A-Bent with regard to S-Bent and Bent.

The previous results suggest that the amount of active sites available for functionalization would not be the limiting factor for the grafting reaction of silane molecules on the surface of the bentonite layers. Therefore, restrictions on conformational requirement and mobility imposed by the clay interlayer could have a more prominent effect on the silylation reaction within the interlayer spaces rather than the amount of –OH groups available for the reaction.

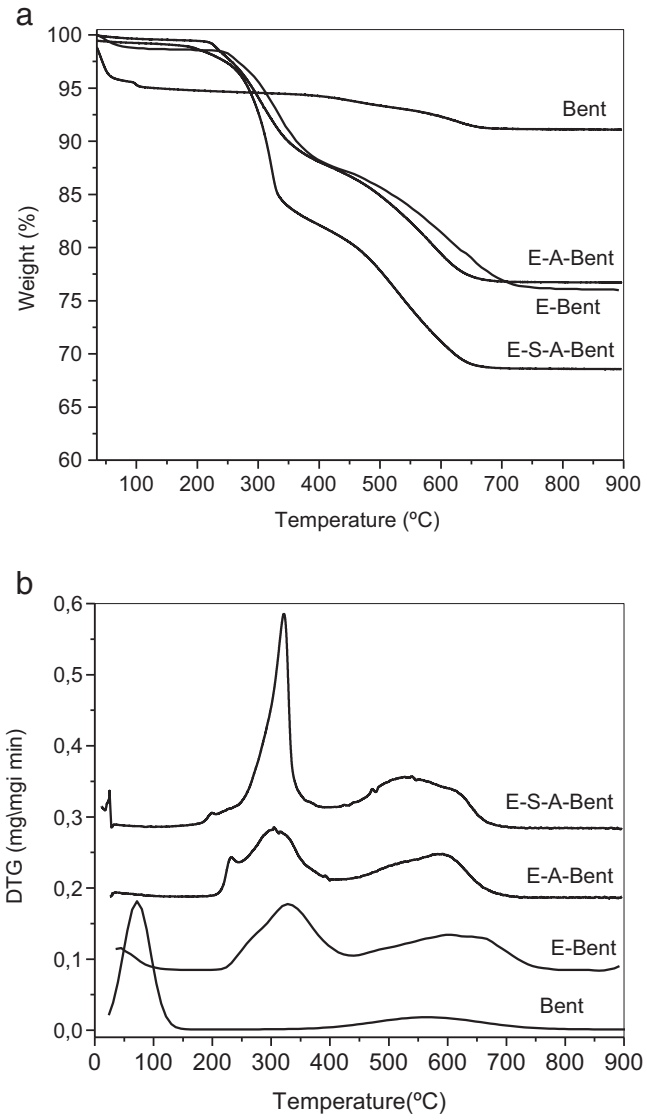

Fig. 5. a. TGA curves of Bent, E-Bent, E–A-Bent and E–S–A-Bent. b. DTG curves of Bent, E-Bent, E–A-Bent and E–S–A-Bent.

3.3. Cationic exchange of acid-activated Bent (E–A-Bent) and silylated acid-activated Bent (E–S–A-Bent)

The cationic exchange reaction is a widely exploited method to increase the compatibility of hydrophilic clay towards organic polymer matrices (Calderon et al., 2008; Picard et al., 2007; Xi et al., 2007). In this kind of reactions, hydrated cations located in the interlayer space are replaced by positively charged surfactants such as alkyl ammonium or phosphonium cations with long alkyl chains. After this treatment, the basal spacing of the layers increases and the modified clay has less surface energy and hence is more compatible with hydrophobic polymers.

In this section, the effect of combining the acid-activation treatment with a cationic exchange reaction is reported. The Bent was first activated by treatment with mineral acid, and then the activated bentonite was further modified by cationic exchange reaction with TBHP. With the aim of analyzing the effect of the acid-activation treatment on the further modification, the cationic exchange reaction was also performed on a natural bentonite sample. The FTIR spectra of the exchanged acid-activated bentonite (E–A-Bent) and the exchanged bentonite (E-Bent) are shown in Fig. 1, and compared with the natural bentonite (Bent). The E–A-Bent and E-Bent exhibit a new absorption peak at 1460 cm^{-1} due to the C – C asymmetric bending of the alkyl chains of TBHP present in the clay. The appearance of strong absorption bands at 2987 and 2900 cm^{-1} assigned to the antisymmetric and symmetric stretching of the methylene groups introduced by TBHP also indicates the existence of phosphonium surfactant in these samples. At the same time, the peaks assigned to the stretching and bending vibrations for the hydroxyl groups of water molecules present in the Bent, at 3440 and 1640 cm^{-1}, are significantly reduced in intensity indicating a less content of water in the E–A-Bent and E-Bent.

The TGA curves of E–A-Bent and E-Bent in comparison with that of Bent are shown in Fig. 5a, whereas the respective first derivatives (DTG) are shown in Fig. 5b. As it can be observed (Fig. 5b), the prominent peak at 70 °C for the Bent, attributed to the loss of physically adsorbed water, is clearly reduced in the E–A-Bent and E-Bent, indicating a less content of water in these samples. These results are in agreement with those obtained by FTIR analysis. In addition, E–A-Bent and E-Bent present significant mass losses in the range from 200 to 450 °C (Fig. 5b), which correspond to the decomposition of the surfactant. The comparison of the TGA curves reveals that there is 18.8 w/w% and 18.4 w/w% of organic content in the E-Bent and E–A-Bent samples

respectively (Table 2), which corresponds to the loss of all the organic cations. It is worth to note that in the range between 200 and 450 °C the DTG curve of E–A-Bent (Fig. 5b) exhibits a second peak at 230 °C which is almost absent in the E-Bent. This mass loss at lower temperature could be related to physically adsorbed surfactant, or to the degradation of surfactant cations that reside exterior to the layers via interaction between the negatively charged sheets and the positive surfactant cations (Kooli, 2008). This result would indicate that the intercalation of TBHP cations in the acid-activated bentonite has not occurred via a simple cation exchange reaction.

Interestingly, the E-Bent and E–A-Bent samples presented a significant reduction in the equilibrium water uptake percentage with respect to the neat Bent sample (Table 2). In fact, the equilibrium water uptake percentage measured for the unmodified Bent (17.4%) was reduced to 3.4% for E–A-Bent, and to 2.8% for E-Bent. This is to say, in the conditions of the experiment, the E–A-Bent and E-Bent samples absorbed 80 and 84% less amount of water than the unmodified clay. These results reveal the marked reduction in the hydrophilic character of the clay after the modification treatments.

The XRD patterns for the E–A-Bent and E-Bent samples are presented in Fig. 3. As it can be seen, the basal spacing of these samples is bigger than that of the neat Bent, indicating that the surfactant has been intercalated into the interlayer space of the bentonite. The basal spacing increased from 1.31 nm for Bent to 2.28 nm for E–A-Bent, and to 2.68 nm for E-Bent. Accordingly, the alkyl chains take the arrangement of a paraffin-type monolayer in the interlayer of E–A-Bent and E-Bent (Hu et al., 2013). It should be noted that even when the total organic content of E–A-Bent and E-Bent is similar, the E-Bent presents a bigger basal spacing. This fact is in agreement with the previous interpretation that the intercalation of TBHP cations in the acid-activated bentonite would not occur via a simple cation exchange reaction, as some fraction of TBHP would reside exterior to the layers without affecting the basal spacing of the clay.

As a last strategy of modification, the cationic exchange reaction was carried out on a bentonite sample previously acid-activated and silylated. The procedure was as follows: the Bent was firstly activated by treatment with mineral acid, then the A-Bent was silylated, and finally the S–A-Bent was modified by cationic exchange reaction. The resulting sample is designated E–S–A-Bent. An alternative sequence could have been: first acid-activation, then cationic exchange and finally silylation. However, when this protocol was carried out partly intercalated surfactants were washed out with butanol used as solvent in the silylation reaction, resulting in a decrease of the organic content in the clay. The FTIR spectrum of the E–S–A-Bent sample is shown in Fig. 1, where the appearance of strong absorption bands at 2987 and 2900 cm^{-1} assigned to the methylene groups introduced by alkyl chains of both, TBHP and DMOCS, indicates the presence of phosphonium surfactant and silane in this sample.

The DTG curve of E–S–A-Bent (Fig. 5b) exhibits a first decomposition peak in the range between 200 and 450 °C due to the decomposition of surfactant and intercalated silane, and a second decomposition step in the range from 450 to 700 °C. At least two overlapped peaks appear in this last range, one of them at around 500 °C attributed to the release of grafted silane, and the other at about 600 °C assigned to the dehydroxylation of the bentonite. The comparison of the TGA curves reveals that there is 26.7 w/w% of total organic content in E–S–A-Bent (Table 2), that is to say 8.3 w/w% more than in E–A-Bent. Taking into account that the organic content of S–A-Bent was 3.5 w/w% (see Table 2), it can be concluded that the treatment of silylation allowed increasing the uptaken amount of surfactant cations during the further cationic exchange reaction.

The XRD pattern for E–S–A-Bent is shown in Fig. 3. The calculated basal spacing for this sample (2.6 nm, see Table 2) was as high as that of E-Bent, and remarkably the equilibrium water uptake percentage measured for E–S–A-Bent (2.6%) was the lowest one of all the treatments considered in the present work.

4. Conclusions

Different strategies of modification of bentonite combining reactions of cationic exchange, silylation and acid activation have been analyzed. The silylated bentonite presented a significant reduction in the equilibrium water uptake percentage with respect to the unmodified clay, even when small amounts of silane are incorporated to the clay. On the other hand, no significant changes in the organic content were obtained when the silylation reaction was performed on previously acid-activated bentonite. This result suggests that restrictions on conformational requirement and mobility imposed by the clay interlayer have a more prominent effect on the silylation reaction within the interlayer spaces rather than the amount of –OH groups available for the reaction.

When a sample of silylated and activated bentonite was further modified by cationic exchange reaction, it was found that the previous treatments allowed in increasing the uptaken amount of surfactant cations during the exchange reaction. In fact, the combination of the three treatments (acid-activation, silylation and cationic exchange) gave place to the modified bentonite with the biggest basal spacing and the lower equilibrium water uptake percentage. This sample can be used as promising filler for the formulation of clay polymer nanocomposites. Work is in progress in this direction.

Acknowledgements

The financial support of the National Research Council (CONICET); PIP 0014 and PIP 0527; the National Agency for the Promotion of Science and Technology (ANPCyT); PICT 1983; and the University of Mar del Plata, Argentina, is gratefully acknowledged.

Appendix A. Supplementary data

Supplementary data to this article can be found online at http://dx.doi.org/10.1016/j.clay.2014.07.002.

References

Alexandre, M., Dubois, P., 2000. Polymer-layered silicate nanocomposites: preparation, properties and uses of a new class of materials. Mater. Sci. Eng. R 28, 1–63.
Bergaya, F., Jaber, M., Lambert, J.-F., 2011a. Clays and Clay Minerals. In: Galimberti, M. (Ed.), Rubber-Clay Nanocomposites: Science, Technology, and Applications. John Wiley & Sons Inc., pp. 1–44.
Bergaya, F., Jaber, M., Lambert, J.-F., 2011b. Organophilic clay minerals. In: Galimberti, M. (Ed.), Rubber-Clay Nanocomposites: Science, Technology, and Applications. Wiley Online Library, pp. 45–86.
Bergaya, F., Jaber, M., Lambert, J.-F., 2012. Clays and clay minerals as layered nanofillers for (bio) polymers. In: Avérous, L., Pollet, E. (Eds.), Environmental Silicate Nano-Biocomposites. Springer, pp. 41–75.
Bergaya, F., Detellier, C., Lambert, J.F., Lagaly, G., 2013. Chapter 13.0 — introduction to clay–polymer nanocomposites (CPN). In: Bergaya, F., Lagaly, G. (Eds.), Developments in Clay Science. Elsevier, pp. 655–677.
Breen, C., Madejová, J., Komadel, P., 1995. Correlation of catalytic activity with infrared,^{29}Si MAS NMR and acidity data for HCl-treated fine fractions of montmorillonites. Appl. Clay Sci. 10, 219–230.
Calderon, J.U., Lennox, B., Kamal, M.R., 2008. Thermally stable phosphonium–montmorillonite organoclays. Appl. Clay Sci. 40, 90–98.
Čapková, P., Pospíšil, M., Valášková, M., Měřínská, D., Trchová, M., Sedláková, Z., Weiss, Z., Šimoník, J., 2006. Structure of montmorillonite cointercalated with stearic acid and octadecylamine: modeling, diffraction, IR spectroscopy. J. Colloid Interface Sci. 300, 264–269.
Chen, G.-X., Yoon, J.-S., 2005a. Nonisothermal crystallization kinetics of poly(butylene succinate) composites with a twice functionalized organoclay. J. Polym. Sci. B Polym. Phys. 43, 817–826.
Chen, G.-X., Yoon, J.-S., 2005b. Thermal stability of poly (L-lactide)/poly (butylene succinate)/clay nanocomposites. Polym. Degrad. Stab. 88, 206–212.
Chen, G.X., Yoon, J.S., 2005c. Clay functionalization and organization for delamination of the silicate tactoids in poly(L-lactide) matrix. Macromol. Rapid Commun. 26, 899–904.
Di Gianni, A., Amerio, E., Monticelli, O., Bongiovanni, R., 2008. Preparation of polymer/clay mineral nanocomposites via dispersion of silylated montmorillonite in a UV curable epoxy matrix. Appl. Clay Sci. 42, 116–124.
Drown, E., Mohanty, A., Parulekar, Y., Hasija, D., Harte, B., Misra, M., Kurian, J., 2007. The surface characteristics of organoclays and their effect on the properties of poly (trimethylene terephthalate) nanocomposites. Compos. Sci. Technol. 67, 3168–3175.

Fernández, M.J., Fernández, M.D., Aranburu, I., 2013. Poly (L-lactic acid)/organically modified vermiculite nanocomposites prepared by melt compounding: effect of clay modification on microstructure and thermal properties. Eur. Polym. J. 49, 1257–1267.
Fornes, T., Yoon, P., Keskkula, H., Paul, D., 2001. Nylon 6 nanocomposites: the effect of matrix molecular weight. Polymer 42, 09929–09940.
Frost, R.L., Mako, E., Kristóf, J., Horváth, E., Kloprogge, J.T., 2001. Modification of kaolinite surfaces by mechanochemical treatment. Langmuir 17, 4731–4738.
Greenspan, L., 1977. Humidity fixed points of binary saturated aqueous solutions. J. Res. Natl. Bur. Stand. 81, 89–96.
He, H., Duchet, J., Galy, J., Gerard, J.-F., 2005a. Grafting of swelling clay materials with 3-aminopropyltriethoxysilane. J. Colloid Interface Sci. 288, 171–176.
He, H., Galy, J., Gerard, J.-F., 2005b. Molecular simulation of the interlayer structure and the mobility of alkyl chains in HDTMA+/montmorillonite hybrids. J. Phys. Chem. B 109, 13301–13306.
He, H., Duchet, J., Galy, J., Gérard, J.-F., 2006. Influence of cationic surfactant removal on the thermal stability of organoclays. J. Colloid Interface Sci. 295, 202–208.
He, H., Tao, Q., Zhu, J., Yuan, P., Shen, W., Yang, S., 2013. Silylation of clay mineral surfaces. Appl. Clay Sci. 71, 15–20.
Hedley, C., Yuan, G., Theng, B., 2007. Thermal analysis of montmorillonites modified with quaternary phosphonium and ammonium surfactants. Appl. Clay Sci. 35, 180–188.
Herrera, N.N., Letoffe, J.-M., Putaux, J.-L., David, L., Bourgeat-Lami, E., 2004. Aqueous dispersions of silane-functionalized laponite clay platelets. A first step toward the elaboration of water-based polymer/clay nanocomposites. Langmuir 20, 1564–1571.
Hu, Z., He, G., Liu, Y., Dong, C., Wu, X., Zhao, W., 2013. Effects of surfactant concentration on alkyl chain arrangements in dry and swollen organic montmorillonite. Appl. Clay Sci. 75, 134–140.
Isoda, K., Kuroda, K., Ogawa, M., 2000. Interlamellar grafting of γ-methacryloxypropylsilyl groups on magadiite and copolymerization with methyl methacrylate. Chem. Mater. 12, 1702–1707.
Komadel, P., Madejová, J., 2006. Chapter 7.1 acid activation of clay minerals. In: Bergaya, F., Theng, B.K.G., Lagaly, G. (Eds.), Developments in Clay Science. Elsevier, pp. 263–287.
Kooli, F., 2008. Exfoliation properties of acid-activated montmorillonites and their resulting organoclays. Langmuir 25, 724–730.
Kristof, J., Frost, R.L., Kloprogge, J.T., Horvath, E., Mako, E., 2002. Detection of four different OH-groups in ground kaolinite with controlled-rate thermal analysis. J. Therm. Anal. Calorim. 69, 77–83.
Lambert, J.F., Bergaya, F., 2013. Smectite–polymer nanocomposites. In: Lagaly, G., Bergaya, F. (Eds.), Developments in Clay Science. Elsevier, pp. 679–706.
Limpanart, S., Khunthon, S., Taepaiboon, P., Supaphol, P., Srikhirin, T., Udomkichdecha, W., Boontongkong, Y., 2005. Effect of the surfactant coverage on the preparation of polystyrene–clay nanocomposites prepared by melt intercalation. Mater. Lett. 59, 2292–2295.
Mandalia, T., Bergaya, F., 2006. Organo clay mineral-melted polyolefin nanocomposites effect of surfactant/CEC ratio. J. Phys. Chem. Solids 67, 836–845.
Mortland, M.M., Shaobai, S., Boyd, S.A., 1986. Clay–organic complexes as adsorbents for phenol and chlorophenols. Clay Clay Miner. 34, 581–585.
Park, K.-W., Jeong, S.-Y., Kwon, O.-Y., 2004a. Interlamellar silylation of H-kenyaite with 3-aminopropyltriethoxysilane. Appl. Clay Sci. 27, 21–27.
Park, M., Shim, I.-K., Jung, E.-Y., Choy, J.-H., 2004b. Modification of external surface of laponite by silane grafting. J. Phys. Chem. Solids 65, 499–501.
Picard, E., Gauthier, H., Gérard, J.-F., Espuche, E., 2007. Influence of the intercalated cations on the surface energy of montmorillonites: consequences for the morphology and gas barrier properties of polyethylene/montmorillonites nanocomposites. J. Colloid Interface Sci. 307, 364–376.
Pinnavaia, T.J., 1983. Intercalated clay catalysts. Science 220, 365–371.
Roelofs, J., Berben, P., 2006. Preparation and performance of synthetic organoclays. Appl. Clay Sci. 33, 13–20.
Tripp, C., Hair, M., 1993. Chemical attachment of chlorosilanes to silica: a two-step amine-promoted reaction. J. Phys. Chem. 97, 5693–5698.
Tunç, S., Duman, O., Kanci, B., 2012. Rheological measurements of Na-bentonite and sepiolite particles in the presence of tetradecyltrimethylammonium bromide, sodium tetradecyl sulfonate and Brij 30 surfactants. Colloids Surf. A 398, 37–47.
Van Olphen, H., 1977. An Introduction to Clay Colloid Chemistry: For Clay Technologists, Geologists, and Soil Scientists. Wiley.
Xi, Y., Ding, Z., He, H., Frost, R.L., 2004. Structure of organoclays — an X-ray diffraction and thermogravimetric analysis study. J. Colloid Interface Sci. 277, 116–120.
Xi, Y., Frost, R.L., He, H., 2007. Modification of the surfaces of Wyoming montmorillonite by the cationic surfactants alkyl trimethyl, dialkyl dimethyl, and trialkyl methyl ammonium bromides. J. Colloid Interface Sci. 305, 150–158.
Xie, W., Xie, R., Pan, W.-P., Hunter, D., Koene, B., Tan, L.-S., Vaia, R., 2002. Thermal stability of quaternary phosphonium modified montmorillonites. Chem. Mater. 14, 4837–4845.
Zampori, L., Gallo Stampino, P., Dotelli, G., Botta, D., Natali Sora, I., Setti, M., 2008. Interlayer expansion of dimethyl ditallowylammonium montmorillonite as a function of 2-chloroaniline adsorption. Appl. Clay Sci. 41, 149–157.
Zhang, J., Gupta, R.K., Wilkie, C.A., 2006. Controlled silylation of montmorillonite and its polyethylene nanocomposites. Polymer 47, 4537–4543.